A Novel Technique to Identify Flow Patterns During Liquid−Liquid Two-Phase Upflow Through Vertical Pipe

ARTICLE *in* INDUSTRIAL & ENGINEERING CHEMISTRY RESEARCH · FEBRUARY 2006

Impact Factor: 2.59 · DOI: 10.1021/ie051257e

3 AUTHORS, INCLUDING:

Arun Jana
Sardar Vallabhbhai National Institute of Tech…
10 PUBLICATIONS **111** CITATIONS
SEE PROFILE

Gargi Das
IIT Kharagpur
57 PUBLICATIONS **578** CITATIONS
SEE PROFILE

A Novel Technique to Identify Flow Patterns during Liquid−Liquid Two-Phase Upflow through a Vertical Pipe

Arun Kumar Jana,[†] Gargi Das,[†] and Prasanta Kumar Das*[,‡]

Department of Chemical Engineering, Indian Institute of Technology, Kharagpur−721302, India, and Department of Mechanical Engineering, Indian Institute of Technology, Kharagpur−721302, India

In the present study, a novel optical technique has been devised for identification of flow patterns during liquid−liquid two-phase upflow through a vertical pipe. It is based on the difference in optical properties of the two phases and estimates the flow patterns on the basis of the proportion of light attenuated and scattered by the two-phase mixture. The nonintrusive measurement system comprises a laser source and a photodiode sensor located on the diametrically opposite position of the test pipe. The light incident on the photodiode is converted to a voltage signal by a processing circuit and recorded in a PC via a data-acquisition system. Two types of statistical analysis, namely, the probability density function analysis and the wavelet resolution technique of the probe signals, have been adopted for a better understanding of the flow phenomena. The distribution has been observed to be bubbly at low flow rates of both the liquids. Core annular flow has been identified at high kerosene velocities. The transition from bubbly to core annular flow occurs through a chaotic distribution of both the liquids where the dominating phase shifts from water to kerosene. This is named as the churn flow pattern. The information thus obtained has been represented as a flow-pattern map. The flow-pattern map has been compared with the existing theoretical and empirical models.

1. Introduction

Liquid−liquid two-phase flows are encountered in a wide variety of applications. They occur in solvent-extraction equipment like column contractors and mixer-settlers. This type of flow has been proposed as a cooling system in a controlled fusion reactor. In the petroleum industry, two-phase oil−water flows are important in production wells and in subsea pipelines. Production of oil from offshore reservoirs also implies the simultaneous production of free water. For many years, the amount of free water produced was small and, hence, given little attention. However, in recent years, water production has increased due to reservoir aging and more-complex reservoirs. Offshore production includes long horizontal pipes for multiphase transport over long distances. The pressure required in transporting the fluids through both horizontal and vertical pipes can significantly be affected by the distribution of the oil and water phases. Understanding the complex nature of oil/water flow is, therefore, important to build predictive design models with high accuracy.

Liquid−liquid flows have thus assumed greater importance in recent years. Unlike gas−liquid two-phase flow, much less is known about the physics of liquid−liquid flow. The studies on liquid−liquid flow are strongly influenced by the approaches used in gas−liquid flow. However, while the latter is characterized by low density and viscosity ratios, in liquid−liquid systems the density ratio is close to unity and the viscosity ratio extends over a wide range of magnitude. Both the liquids can also wet the conduit wall. As a result, the liquid−liquid systems may behave differently from the gas−liquid cases. In general, the gas−liquid results cannot be extended for the prediction of liquid−liquid flows.

In the early years of investigation, visual observation and photography-related techniques were used for detection of flow pattern in liquid−liquid flows.[1−5] For this, they allowed the liquid mixture to flow through a transparent pipe or through a transparent window on the pipe wall. It was reported that the photographic techniques, including high-speed photography or videography, are often not sufficient to give a clear image of the distribution of the phases.[6] To overcome the problem, researchers have adopted several objective techniques. Vigneaux et al.[7] used a high frequency (1 GHz) impedance probe to measure the distribution of the water volume fraction across a pipe cross section for oil−water flow. Angeli and Hewitt[6] determined the local phase fraction in oil−water flow through a horizontal pipe with a high-frequency impedance probe and detected the continuous phase in dispersed flows with a needle-type conductivity probe. Jin et al.[8] used a wall-mounted ring electrode probe and characterized the flow patterns in oil/water two-phase flow in a vertical pipe. The authors analyzed the fluctuating conductance time-series signals using fractal, chaos, and Kolmogorov entropy. Ioannou et al.[9] applied a conductivity probe to monitor the change of the continuous phase and an impedance probe to measure the volume fraction distribution near the phase-inversion point in a horizontal pipe. Lovick and Angeli[10] identified the dual continuous flow-pattern boundaries with the use of impedance and conductivity probes described in ref 9. Ioannou et al.[11] used three impedance ring probes along the pipe to investigate whether phase inversion happens simultaneously in the whole test section. Recently, Jana et al.[12] have adopted three different designs of conductivity probes to identify the flow patterns during kerosene−water upflow through vertical pipes. They performed the probability density function (PDF) analysis and wavelet resolution of the random signals and identified the presence of kerosene dispersed in water, bubbly flow at low kerosene velocities, and core annular flow at high flow rates of the oil phase. A limited number of efforts have been made to develop a phase-detection probe for liquid−liquid flow using techniques other than the conductivity or impedance principle. Farrar and Bruun[13] applied a hot film

* Corresponding author. Tel.: +91-3222-282916. Fax: +91-3222-255303. E-mail: pkd@mech.iitkgp.ernet.in.

[†] Department of Chemical Engineering, Indian Institute of Technology.

[‡] Department of Mechanical Engineering, Indian Institute of Technology.

10.1021/ie051257e CCC: $33.50
Published on Web 02/24/2006

anemometer based technique in the study of kerosene−water two-phase flow in the bubbly, spherical cap bubble and churn flow regimes. The authors have presented a radial bubble volume fraction profile, a bubble cut chord length profile, a bubble mean velocity profile, and a turbulent intensity profile. Hamad and co-workers[14,15] developed an intrusive needle-type optical probe to study kerosene−water two-phase flow through a vertical pipe. The probe utilizes light emitted inside an optical guide. The intensity of the light reflected back from the probe tip depends on the surrounding medium and is used for phase detection. Simmons and Azzopardi[16] have utilized laser diffraction and backscatter techniques to study drop size in kerosene and aqueous potassium carbonate solution for both vertical upflow and horizontal pipes.

The above survey reveals that most of the studies on liquid−liquid two-phase flows have adopted the conductivity probe technique, and most of the probes adopted are intrusive in nature. As a result, they get wet by the oil phase during measurement. This greatly alters the response. Moreover, the difference in conductivity between two phases for liquid−liquid systems is less than that for a gas−liquid system. Angeli and Hewitt[6] have further reported that the conductivity probe is effective in a water continuous phase, and a few researchers[9,10] have used a conductivity probe along with an impedance probe during liquid−liquid flow measurement.

By judging the limitation of conductivity probes in liquid−liquid two-phase flows and the inadequacy of conductivity probes and the nonavailability of other techniques for phase identification of oil−water flow, there is always a scope of developing new instrumentation methods. In the present study, an effort has been made to develop a simple, nonintrusive measurement system to identify the flow patterns in liquid−liquid two-phase upflow through a vertical pipe. A novel optical probe based on the difference in optical properties of the two liquids has been devised for this purpose. It estimates the different flow patterns on the basis of the proportion of light attenuated and scattered by the two-phase mixture. Attempts have next been focused to represent the flow-pattern data thus obtained in the form of a flow-pattern map. The flow-pattern map has been compared with the empirical and theoretical models reported in the literature for predicting the transition between different flow patterns. It is interesting to note that several researchers[9−11] have reported a unique phenomenon during liquid−liquid flows. They have observed that the continuous phase shifts from oil to water or vice versa under certain conditions. This has been termed as "phase inversion". Several empirical correlations have been proposed in the literature to predict phase inversion during liquid−liquid flows through horizontal pipes and stirred vessels. Brauner and Ullmann[17] have also presented a theoretical analysis on the principle of minimization of total energy to predict phase inversion during oil−water horizontal flows. Since the analysis has been observed to be independent of conduit orientation, we were interested in superimposing the predictions of the available models in the present flow-pattern map. The region of existence of phase inversion under the conditions of the present study has been observed to understand the physics underlying the phenomena.

2. Experimental Setup and Procedure

The schematic diagram of the setup is shown in Figure 1. The details of the experimental setup and procedure are mentioned in Jana et al.[12] It consists of a test rig and accessories, namely, water tank, kerosene tank, kerosene−water separator, two centrifugal pumps, and measuring equipment. The test section comprises a vertical transparent acrylic resin tube of 0.0254 m diameter and 1.5 m length. Acrylic resin was selected as the material of construction to enable visual observation of the flow phenomena. The transparent tube also facilitates the optical measurements. The test section is preceded by an entry length of 2.0 m to ensure fully developed flow and followed by an exit length of 0.60 m to avoid any flow disturbance in the test rig. A glass view box (VB) is attached to the test section for photography. The fluids selected are water and dyed kerosene. Their physical properties are given in Table 1. Blue-dyed kerosene has been used in the experiments for better visualization of the flow. It also ensures a wide difference in the optical properties of the two phases.

The two liquids, after being pumped through previously calibrated rotameters, are introduced to a T-mixer at the entry. The water and oil enter from the vertical and horizontal directions, respectively. After passing through the test section, the two-phase mixture enters a separator, where the two phases are gravity separated and directed to their respective storage tanks.

The superficial velocities of both liquids have been varied from 0.05 to 1.5 m/s. The experiments are carried out by increasing kerosene velocity at a constant water velocity. The water velocity is then changed for the next set of experiments. The entire test runs have been repeated a number of times to ensure reproducibility.

2.1. Measurement Technique. The present method uses an optical technique to identify flow patterns in liquid−liquid systems on the basis of the difference in optical properties of the two liquids. A detailed diagram of the optical probe system is depicted in Figure 2. It comprises a point semiconductor laser source (∼2 mW, ∼660 nm wavelength, and 2 mm beam diameter), which serves as a source of monochromatic laser light. A photodiode sensor (SD 3410, manufactured by Honeywell) is located at the diametrically opposite point to detect light transmitted by the laser source after its passage through the test section. The operating temperature of the sensor ranges from −55 to 125 °C. It is placed inside a dark box to ensure that light only from the laser source, and not from any other external agency, falls on it. The narrow laser beam passes through the two-phase medium before falling on the photo detector. On its path from the source to the detector, it has to pass through two different phases and an ensemble of interfaces created by bubbles, drops, waves, etc. These ensembles are the characteristics of a particular flow regime and may change with space and time. However, averaged over a time scale as well as over a diametral plane, this presents a steady feature. Light passing through a two phase-medium undergoes different interactions, namely, reflection, refraction, absorption scattering, etc. The intensity of the light, which will fall on the detector, depends on the interactions, which in turn are dependent on the phase content and interfacial configuration characterizing a particular flow pattern.

The light incident on the photodiode is converted to a voltage signal. This is amplified by an indigenously made amplifier circuit and recorded continuously as time-series data in a computer through a data acquisition/switch unit (Agilent 3970A) with a frequency of 25 Hz over a period of 100 s. The signal depicts the variation in the intensity of light falling on the diode. Initially, the signals have been recorded during flows of single-phase water and kerosene, respectively. The results have indicated a single steady voltage for each phase. Measurements with different flow rates of either of the liquids have yielded

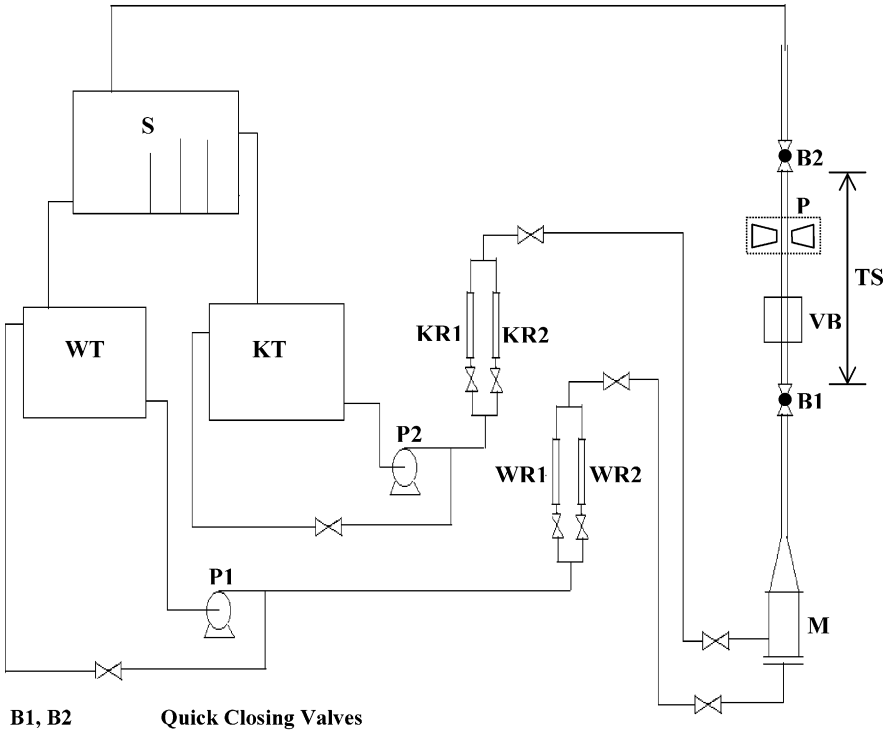

Figure 1. Schematic diagram of experimental setup.

Table 1. Physical Properties of Water and Kerosene (at 30 °C and Atmospheric Pressure)

fluid	density (kg/m^3)	viscosity ($N\ s\ m^{-2}$)	surface tension (N/m)
kerosene	792	0.00137	0.027
water	1000	0.001	0.072

the same voltage value, irrespective of velocity. Because of the higher absorption coefficient of kerosene, the voltage obtained is higher for water as compared to kerosene.

During two-phase flow, the amount of light incident on the photodiode mainly depends on the fraction absorbed and scattered by the flowing mixture. The amount of attenuation increases with the increase in the kerosene fraction in the pipe. Apart from attenuation, scattering becomes predominant with the onset of the droplets and wavy interfaces. The optical probe has been observed to be a very effective tool to identify the flow patterns and transitions, not only on the basis of the relative proportion of the two phases in the conduit but also from the fraction of light attenuated and scattered by the distribution of the two phases.

The main advantage of the probe is that it is nonintrusive, and the question of wetting the probe by the oil phase or obstruction to flow has been nullified. The device is reliable and inexpensive. The coherence character of the laser light enables a better penetration through the fluids, and a high sensitivity of the photodiode makes the response of the system extremely fast. Thus, it provides an instantaneous response as well as a good spatial resolution. Moreover, it is small in size,

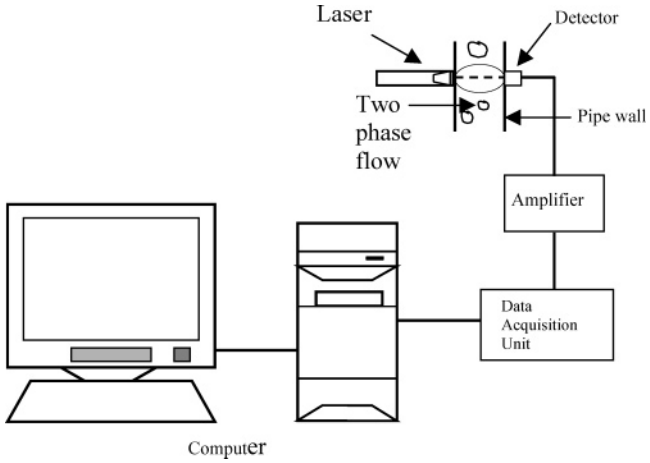

Figure 2. Optical probe system.

it is easy to handle and use, and the components required are easily available. It is based on the difference in optical properties of the two fluids. Because the probe does not touch the liquid, it is not affected by the individual physical properties of the liquid like corrosiveness, acidity, alkalinity, etc. It has been tested for both liquid−liquid and gas−liquid systems and can be extended to any two-phase flow provided none of the phases are opaque.

2.2. Method of Analysis. Apart from visual observations of the random signals, different statistical analyses of the normalized time-series data have been carried out to get better

information about the phase distribution in the pipe. The probability density function (PDF) and the wavelet analysis have been adopted for this purpose.

2.3. PDF Analysis. The PDF is a well-established technique for the time-series analysis of random signals. It gives the time-averaged histogram depicting the distribution of amplitudes of the signal. Several researchers[18−20] have adopted the technique for identifying flow patterns during gas−liquid flows. Jana et al.[12] have used the method for analysis of conductivity probe signals during liquid−liquid flows. The details of the analysis have been provided in Jones and Delhaye.[18]

The PDF curves have been quantified by means of the statistical moments, namely, median, variance, skewness, and kurtosis. The skewness (third moment) and kurtosis (fourth moment) are nondimensional moments, in contrast to the median and the standard deviation (σ), which has the same dimension as the measured quantities. The skewness is the degree of asymmetry of the distribution of the data. A positive (negative) value of the skewness implies a distribution with a higher number of large (small) values of the parameter than would be expected for a Gaussian distribution. The kurtosis is the degree of peakedness of a distribution. A larger kurtosis depicts a more-peaked distribution.

2.4. Wavelet Analysis. The wavelet transform (WT) is a newly developed time-frequency analysis method, which has good time resolution at high frequencies and good frequency resolution at low frequencies. In principle, wavelets are the building blocks of wavelet transforms, just as trigonometric functions in Fourier transform. In this way, a family of scaled and translated wavelets is created, which can catch different frequency information contained in a time series. Because of the fact that each wavelet is a sort of band-pass filter, the original signal can be used for decomposition of the original time series into different frequency bands, thus allowing a multiresolution analysis of the signal.

Wavelet analysis could be a powerful tool to analyze multiphase systems, which are not only nonlinear but also possess a large number of frequencies because of the inherent randomness of the phenomena. A number of researchers[21−24] have adopted this analysis to understand the hydrodynamics of fluidized beds. A review of the application of the wavelet analysis in different multiphase systems has been given by Drahos et al.[25] Jana et al.[12] have reported considerable success in applying the wavelet analysis to conductivity probe signals for understanding the physics of liquid−liquid flows.

Accordingly, the Daubechies 4 wavelet analysis has been used in the present study. The details of the calculation have been provided by Takei et al.[26] For all wavelet analysis, Matlab with its toolbox has been used. The inherent structures of the different flow patterns and their changes with superficial velocities have been visualized from the decomposed signal.

3. Results and Discussions

Experiments have been performed for superficial velocities of both water and kerosene ranging from 0.05 to 1.5 m/s. To facilitate a comparative study under different flow conditions, the voltage signals are normalized by V_{max}, the voltage obtained when single-phase water passes through the test section.

Initially, experiments are carried out at low water velocity. The kerosene velocity is varied from a low to a high value, keeping the velocity of water constant. The water velocity is then increased to a higher value, and the experiments are repeated for the entire range of kerosene velocity. The fluctuating signals thus obtained are the time series in voltage, and they give qualitative information regarding the chordal average phase distribution across a pipe cross section.

3.1. Estimation of Flow Patterns from Probe Signals and Their PDF Analysis. The flow situation as observed visually and from probe signals and the corresponding PDF curves are depicted in a tabular form in Figures 3−5. In the figures, U_{SW} and U_{SK} denote superficial velocities of water and kerosene, respectively. Each table represents the flow patterns at different constant values of water velocity. The rows of the tables are numbered as 3.1, 3.2, etc. They depict the flow situations for different kerosene velocities at the constant value of water superficial velocity. The depiction is represented in three parts: (a), (b), and (c), denoting the physical appearance of the phase distribution, the probe signals, and the corresponding PDF curves, respectively. The moments of the PDFs are included in the last column (c) of the table for quantification of the PDFs. In this column, the standard deviation, skewness, and kurtosis are denoted by σ, S, and K, respectively.

Figure 3 shows that, at low velocities of the two liquids (U_{SW} = 0.05 m/s and U_{SK} = 0.05 m/s), kerosene is distributed as discrete droplets in water. Most of the droplets have been observed to be cap shaped or spherical. The corresponding probe signals show high fluctuations, with most of the spikes directed toward lower values of V/V_{max}. The effect probably arises because of scattering of light by the kerosene drops. The corresponding PDF is unimodal with a peak at a high value of voltage, a large spread about the peak, and a skewness toward a lower voltage value. This indicates the existence of water as the continuous phase and a dispersion of kerosene drops in it. The configuration has been named as the bubbly flow pattern in agreement to the nomenclature used for gas−liquid cases.

An increase in kerosene superficial velocity (from 0.05 to 0.11 m/s) results in increased size of kerosene drops. They are now slightly longer and irregular shaped, as shown in Figure 3.2a. The increased proportion of kerosene in the flow passage results in a lower average value of V/V_{max} as compared to the previous case. The corresponding PDF curve remains unimodal with the peak shifted to lower values of V/V_{max}, and it still exhibits negative skewness. This confirms that, although water is the continuous phase, there is an increase of kerosene in the flow passage.

A completely different situation arises on a slight increase in kerosene superficial velocity from 0.11 to 0.18 m/s. Here, the entire flow passage appears blue in color and the distribution of the phases cannot be observed from the photographs. The probe gives a completely random signal, and the situation can best be understood by noting the change in the nature of the PDF. An abrupt shift of the PDF curve to a lower value of V/V_{max} ($V/V_{max} < 0.5$) along with a change in sign of the skewness from negative to positive value marks the flow distribution. The standard deviation also becomes higher. This probably hints at a chaotic distribution and a shift of the continuous phase from water to kerosene. Such a shift has been observed by several researchers during liquid−liquid flows through a horizontal pipe[9−11] as well as for liquid−liquid systems in stirred vessels.[27−31] They have termed it "phase inversion", during which oil dispersions in water change over to water dispersed in oil and vice versa. It may be noted that, although the PDF denotes a change in the continuous phase from water to kerosene, it provides no further information about the interfacial configurations.

A further increase in kerosene superficial velocity to 0.25 m/s results in a further decrease in the average value of the signal voltage. The signal has a base value at low V/V_{max} ($V/$

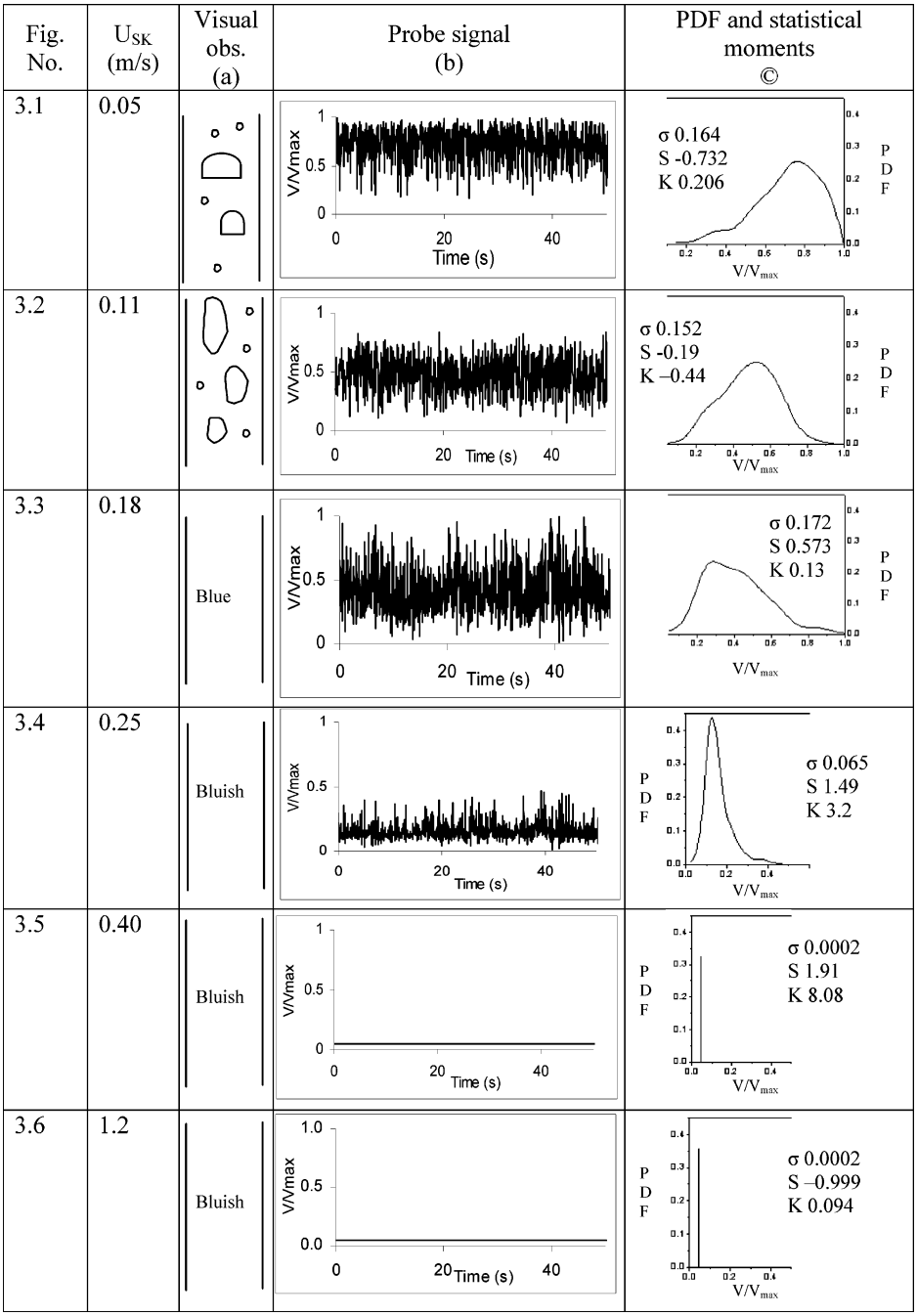

Figure 3. Visual observations, probe signals, and PDFs at $U_{SW} = 0.05$ m/s.

$V_{max} < 0.2$) with the spikes pointing toward higher voltage values. The PDF curve (Figure 3.4c) is unimodal at lower voltage. The spread of the PDF curve decreases abruptly, but the skewness remains positive. This suggests that kerosene is the dominating liquid in the pipe. However, it does not give any idea regarding the distribution of water in the kerosene medium.

With a further increase in the kerosene velocity, the probe signals become practically a straight line and the corresponding PDF curves are also straight lines with negligible spread. The nature of the signal appears similar to that obtained for smooth stratified flow in horizontal pipes. This suggests that the distribution is probably a separated flow pattern with minimum interfacial waviness (minimum scattering) and a large proportion of kerosene (high attenuation of light). A possible configuration may be kerosene flowing as the continuous phase with water shifted to occupy the annular space between the kerosene core and the tube wall rather than being dispersed in the oil. Such a distribution has been termed the "core annular flow pattern" by several researchers[12,32] in the past. Henceforth, the probe signals and the corresponding PDFs remain unaffected with a further increase in kerosene velocity.

Similar trends are observed at higher water velocities. One representative case at a water superficial velocity of 0.3 m/s is depicted in Figure 4. Here, at a low kerosene superficial velocity, the probe signal is at V/V_{max} close to 1. The corresponding PDF curve is unimodal with negative skewness. It may be noted that an increase in the water superficial velocity from 0.05 to 0.3 m/s has shifted the mean value of the PDF to higher values of V/V_{max} as expected. The PDF spread has also decreased as compared to that obtained at a water superficial velocity of 0.05 m/s. This is due to the fact that, at a low water flow rate, kerosene appears as discrete large drops, while at a higher water superficial velocity, the size and frequency of the kerosene drop

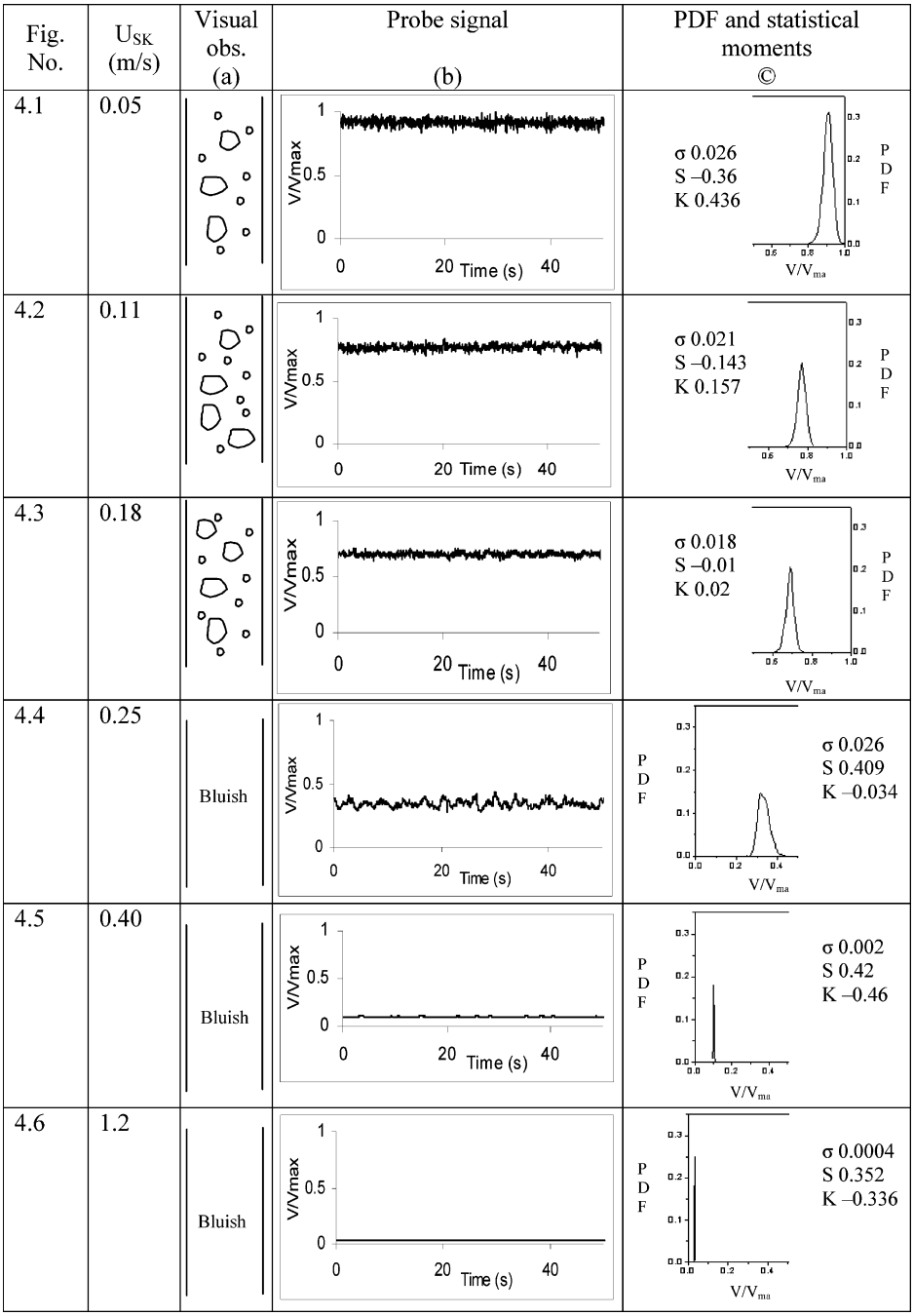

Figure 4. Visual observations, probe signals, and PDFs at $U_{SW} = 0.3$ m/s.

decreases. Their residence time is also much less. With an increase in kerosene superficial velocity, the PDF curve shifts to a lower value of V/V_{max}. The magnitude of skewness as well as the standard deviation decreases while the sign of the skewness remains negative. This continues till a kerosene superficial velocity of 0.18 m/s. At a kerosene superficial velocity of 0.25 m/s, the PDF curve shifts abruptly to $V/V_{max} < 0.5$ with a change in the skewness from negative to positive. The standard deviation increases, which is also reflected in the increased spread of the PDF curve in Figure 4.4. On further increase in kerosene superficial velocity, the probe signal appears smooth. The corresponding PDF curve has negligible spread and shifts to a lower value of voltage ($V/V_{max} \leq 0.1$). The standard deviation gradually decreases, and the PDF curve appears to be practically a straight line with minimum spread. This is similar to the observations presented in Figure 3 at low water velocities.

Thus, it is observed that, at low velocities of water (Figures 3 and 4), the bubbly flow pattern is characterized by a unimodal PDF where the peak increases with an increase in water flow rate. Moreover, the peak appears to shift to higher values of V/V_{max} and the spread decreases. This arises because of the increase in the proportion of water in the pipe and a decrease in the size of the bubbles. The visual appearance of the flow passage and the probe signals also confirms this fact.

On the other hand, as the water flow rate is increased further (Figure 5), the PDF curve is characterized by a shift of the peak slightly toward the left and an increase in the standard deviation of the curve. The flow passage under these conditions appears to be light blue, and a dense cluster of small blue droplets appears to traverse through the pipe at a high velocity. This suggests a more mixed character of flow, leading to a shift of the overall voltage toward lower values. This distribution has been named the "dispersed bubbly flow pattern" in order to

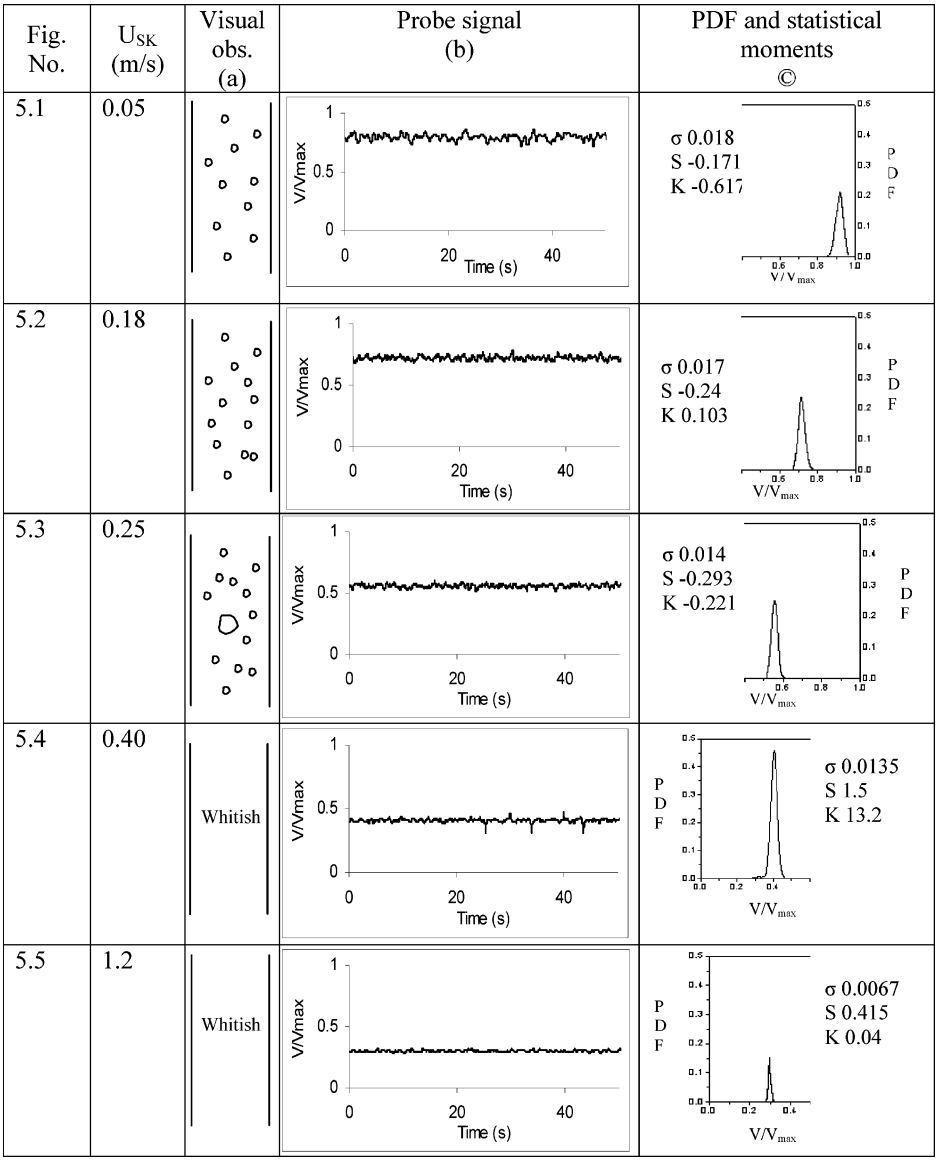

Figure 5. Visual observations, probe signals and PDFs at $U_{SW} = 1.2$ m/s.

distinguish it from bubbly flow pattern at low water flow rates. The visual appearance and probe signals appear to be less effective at higher kerosene velocities under these conditions. The PDF curve shows a shift to lower values of V/V_{max} accompanied by a change in the sign of its skewness above a certain kerosene velocity and, finally, an almost straight-line PDF with negligible spread at still higher kerosene flow rates showing the onset of the "core annular flow".

The above observations thus show the presence of the bubbly flow pattern at low phase velocities and a shift to the dispersed bubbly flow pattern at higher water velocities ($U_{SW} > 1$ m/s). The transition from bubbly to dispersed bubbly is characterized by a shift of the PDF to lower voltage values despite the higher water velocities under these conditions. The distribution at higher kerosene velocities could not be definitely established from the PDF curves. The termination of the bubbly flow pattern is marked by a shift of the PDF to $V/V_{max} < 0.5$ and a change in the sign of the skewness from negative to positive. This probably suggests a change of the dominant phase from water to kerosene. Subsequently, an increase in kerosene velocity results in an almost straight-line PDF with negligible standard deviation at $V/V_{max} < 0.1$. It was expected that water would be dispersed in the continuous oil phase under these conditions. However, the nature of the PDF does not support such a configuration. On the contrary, it suggests a separated nature of flow with kerosene flowing as the continuous phase and water as a film along the wall rather than being dispersed in the oil phase. To understand the detailed distribution of the two phases, further attempts have been made to perform the wavelet analysis of the random signals.

3.2. Wavelet Analysis. The wavelet analysis has next been performed to supplement the information obtained from PDFs under different flow conditions. Since the analysis can decompose a signal into different frequency bands with different time resolutions, it is expected to yield additional information about the interfacial configurations. As mentioned earlier, the Daubechies 4 wavelet analysis has been used to decompose the normalized probe signals into five levels, each with a different frequency band. d_1 reflects the smallest scale and the highest frequency band; d_2, d_3, etc. represent progressively lower frequency bands; and the approximation, a_5, reflects the large-scale resolution.

In our study, we have primarily concentrated our attention on d_1 and a_5 in order to understand the fluctuations due to passing droplets and wavy interfaces, respectively. It is expected that the high-frequency fluctuations will be caused by the

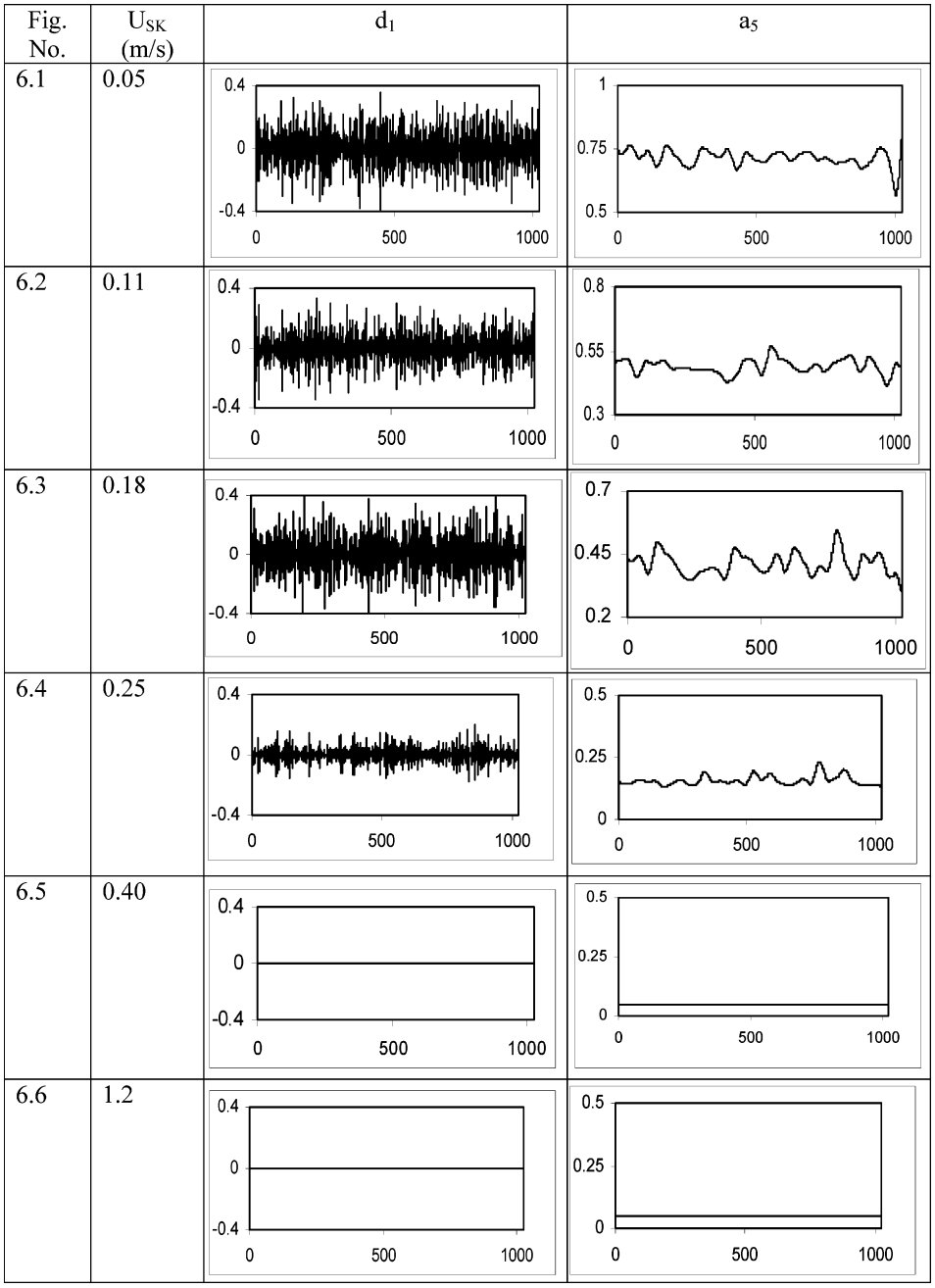

Figure 6. d_1 and a_5 from wavelet analysis of probe signal at $U_{SW} = 0.05$ m/s.

passage of droplets, while the large-scale, low-frequency fluctuations will arise from any waviness of the continuous interface. Accordingly, the d_1 and a_5 components of the normalized probe signals reported in Figures 3−5 are presented in Figures 6−8, respectively.

Figure 6.1 shows that, in the bubbly flow pattern, at low phase velocities, there are large fluctuations in the high-frequency detail d_1. As the kerosene velocity is increased, the bubbly flow pattern (Figures 6.2 and 6.3) is denoted by an increase in the low-frequency, high-resolution a_5, while the fluctuations in d_1 are relatively unchanged. This shows that the increase in the standard deviation of Figure 3.3 occurs because of an increase in the interfacial waviness, probably due to droplet coalescence rather than to an increase in the frequency of dispersion. A further increase in the kerosene flow is marked by an abrupt decrease in the fluctuations at both levels. However, the reduction in the d_1 fluctuations is more pronounced as compared to those of a_5, and finally, both signals are undulating straight lines. This confirms our supposition that the flow at high kerosene velocities is separated flow with a decrease in interfacial waviness at higher oil velocities. A separated flow in the vertical configuration suggests an annular flow pattern with kerosene in the core and water as the film.

The same trend has also been observed at higher water velocities (Figures 7 and 8). In all cases, the bubbly flow pattern is denoted by fluctuations in the d_1 signal where the fluctuations decrease with an increase in the flow rates of either of the phases. The transition from the bubbly flow pattern is marked by an increase in the oscillations of a_5 (Figure 7.4). Subsequently, the oscillations in both levels decrease, but the decrease in the d_1 fluctuations occurs before the a_5 signal levels out. In all the figures, the transition from the bubbly flow pattern is marked by the highest oscillation in a_5 and the flow at higher kerosene velocities has straight-line signals for both d_1 and a_5. The dispersed flow pattern is marked by lower fluctuations in d_1 (Figure 8) as compared to those for bubbly flow. This

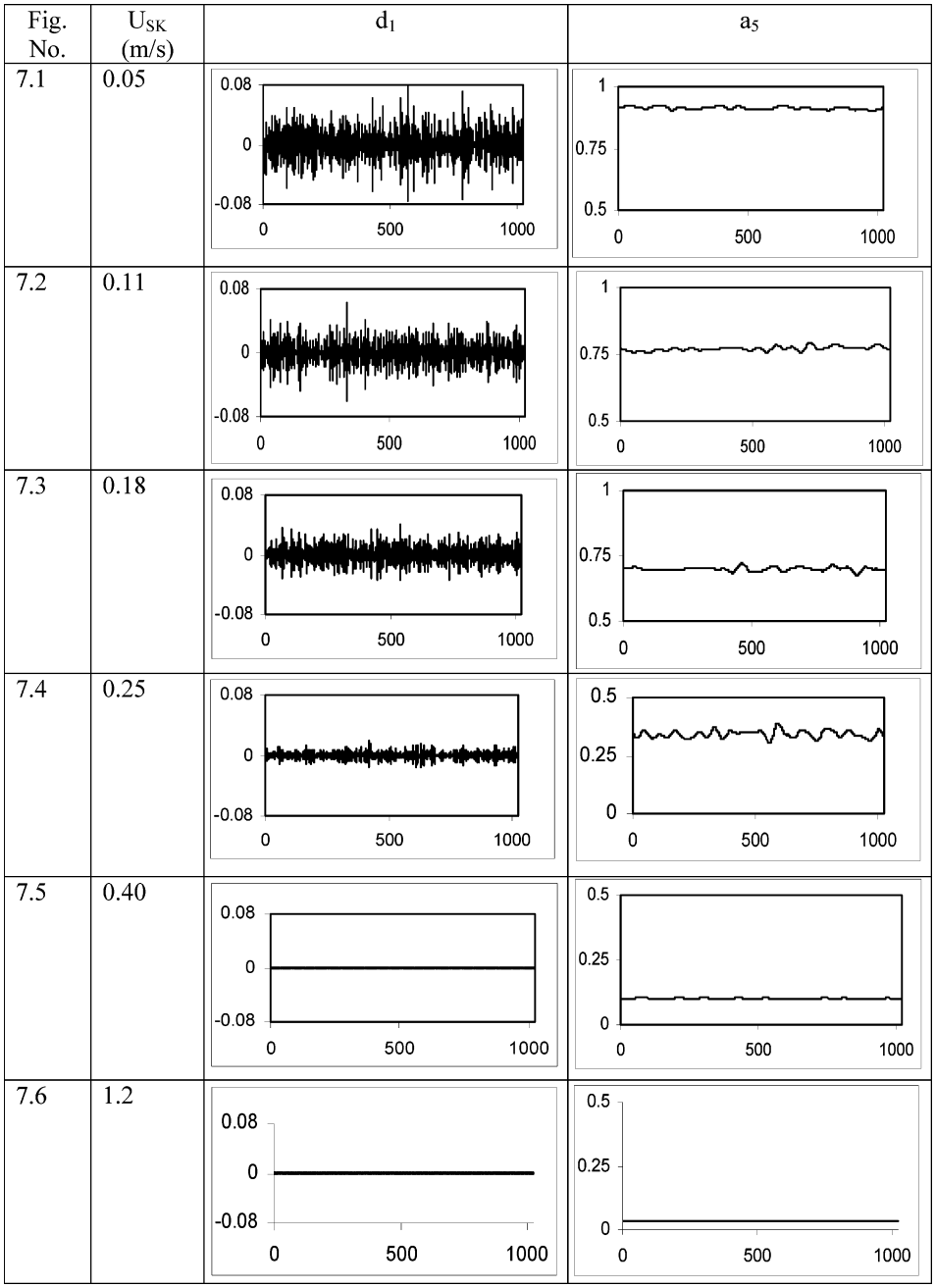

Figure 7. d_1 and a_5 from wavelet analysis of optical probe signal at $U_{SW} = 0.3$ m/s.

explains the smaller value of the standard deviation of the PDF under these conditions. It hints a smaller residence time and size of the bubbles at higher water velocities.

Thus, the wavelet analysis has confirmed that the flow is bubbly at low water velocities and dispersed bubbly under high water flow rates ($U_{SW} > 1$ m/s). The flow is core annular at high kerosene velocities. The region between bubbly and core annular is marked by a chaotic distribution of the two phases with continually changing interface and a shift of the dominating phase from water to oil. This resembles the churn flow pattern of gas−liquid systems.

3.3. Flow-Pattern Map. The information thus obtained from the PDF and wavelet analysis of the random signals is represented graphically as a flow-pattern map (Figure 9). The superficial velocities of the oil and water phases have been chosen as the axes of the map. The choice of the axes has been made in accordance to the choice for gas−liquid flows. The figure shows that the flow is bubbly at low phase velocities. The droplets decrease in size and become finely dispersed at higher water superficial velocities ($U_{SW} > 1$ m/s) because of the shearing force created by the increased turbulence of the water phase. This is termed the "dispersed bubbly flow pattern".

At high kerosene velocities, the rapid coalescence of the oil chunks form a continuous core, which pushes the water to flow as an annular film along the walls. This leads to the core annular flow pattern as also noted by Jana et al.,[12] by adopting different designs of the conductivity probe. The transition between bubbly and core annular flow patterns appears to occur through a phase distribution, which resembles the chaotic and irregular churn flow pattern of gas−liquid flows.

3.4. Comparison of Flow-Pattern Map with Existing Models. Attempts have next been focused on comparing the flow-pattern map thus obtained from optical probe signals and its analysis with the existing models in the literature. It has been noted that the majority of the studies, both theoretical and empirical, are primarily confined to horizontal pipes, but the

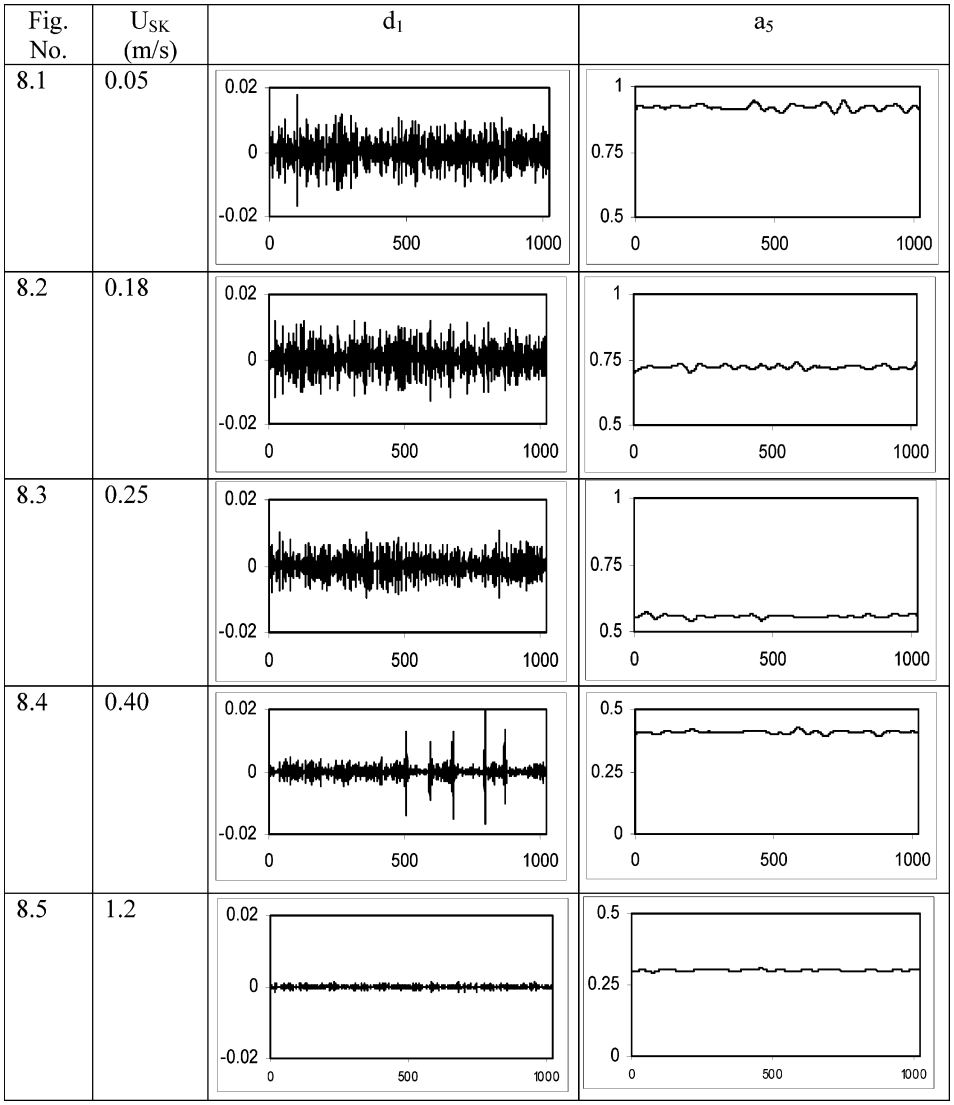

Figure 8. d_1 and a_5 from wavelet analysis of optical probe signal at $U_{SW} = 1.2$ m/s.

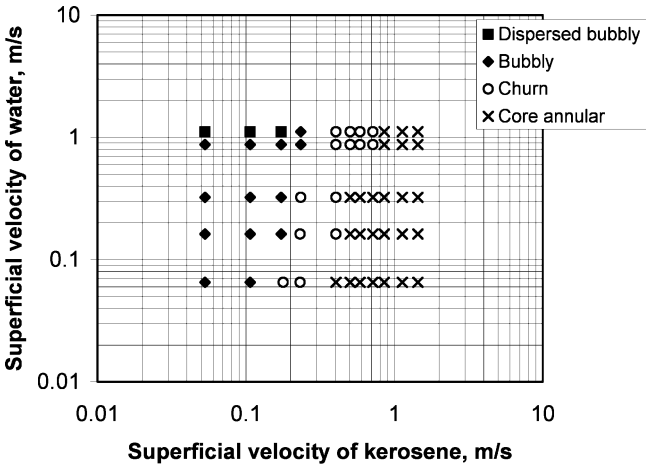

Figure 9. Flow-pattern map.

relationships are not influenced by conduit orientation. So the following analysis has been compared with the flow-pattern map of the present work.

(1) Brauner[33] has reported that the dispersed/intermittent transition is characterized by $\epsilon = 0.2-0.3$, where ϵ is the ratio of the oil superficial velocity to the mixture velocity (oil and water). Beretta et al.[34] have applied this correlation in their flow-pattern map and reported satisfactory results when the mean value of ϵ is taken as 0.24.

(2) Brauner[33] has also proposed the following correlation for the transition from intermittent to annular flow during laminar flow of the two liquids in a horizontal pipe.

$$U_{SO} = \frac{2 + k + \sqrt{(2+k)^2 - 4}}{2} U_{SW} \qquad (1)$$

where $k = \mu_w/\mu_O$ and μ_w and μ_O are the viscosities of water and oil, respectively.

(3) Further, Brauner[35] has adopted the homogeneous model to predict the transition from the bubbly to the dispersed bubbly flow pattern for all pipe inclinations from horizontal to vertical.

The prediction of the above three models under the present flow condition is depicted in Figure 10. The bubbly-to-dispersed bubbly transition as predicted by the model of Brauner and Ullmann[17] is close to the experimental results in the range of the flow conditions studied.

The model for dispersed-to-intermittent transition is close to the present flow-pattern map only at a higher water flow ($U_{SW} > 0.9$ m/s), where ϵ is between 0.2 and 0.3 and deviates significantly at low phase flow rates. It is not a constant at 0.24 as taken by Beretta et al.[34] In the present study, ϵ was observed to be a weak function of U_{SW} for the transition of bubbly to

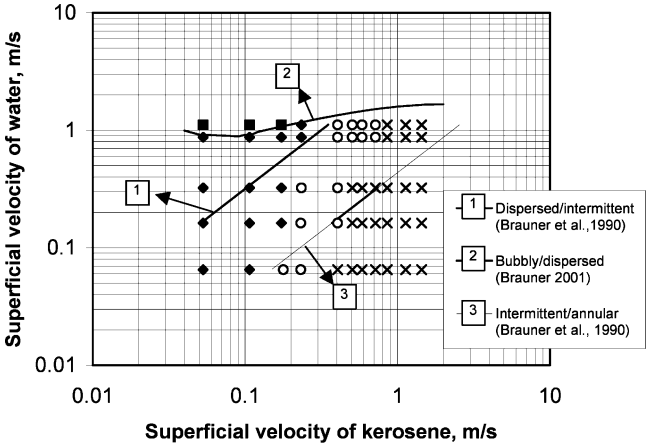

Figure 10. Comparison of flow-pattern map with models.

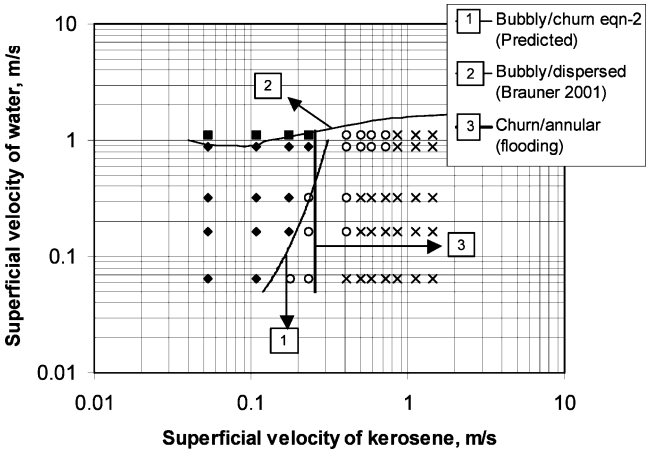

Figure 11. Flow-pattern map and transition boundary.

churn flow pattern, and this is described by the following equation.

$$\epsilon = 0.2103 U_{SW}^{-0.522} \tag{2}$$

The correlation (eq 1) for the transition from intermittent to annular flow pattern does not predict well except for a narrow range of water flow rates for the transition of churn to core annular flow pattern in the present study. This can be attributed to the fact that the analysis has been developed for laminar flow of the two liquids. On the other hand, the transition appears to be governed by the phenomena of flooding as proposed by Wallis.[36] The criterion is given by

$$0.5 < U_{SK}^{*} < 1 \tag{3}$$

where the dimensionless superficial velocity of kerosene (U_{SK}^{*}) according to Wallis[36] is

$$U_{SK}^{*} = U_{SK}\rho_K^{1/2}[gD(\rho_W - \rho_K)]^{-1/2} \tag{4}$$

In eq 4, ρ_K and ρ_W are the densities of kerosene and water, respectively, and D is the pipe diameter. This is obtained by replacing the properties of air with kerosene. The onset of core annular flow pattern is predicted well by flooding, particularly at low water velocities, and this is depicted in Figure 11.

3.5. Comparison with Phase-Inversion Models. Another interesting phenomenon in liquid−liquid flows is phase inversion, where the continuous phase changes to the dispersed phase and vice versa under certain conditions. This phenomenon has

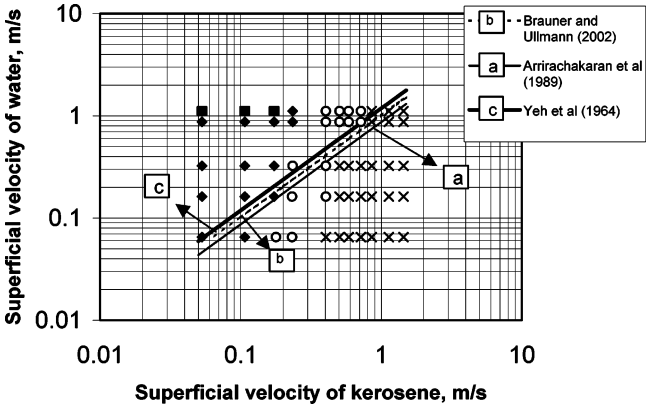

Figure 12. Comparison of flow-pattern map with phase-inversion models.

been reported by several researchers for liquid−liquid systems in horizontal pipes[9−11] and stirred vessels.[27−31] However, no studies have, to date, been performed for vertical pipes. In the present flow condition, the presence of this phenomenon has not been observed. So we were interested in the present work to investigate the location of the phase-inversion curves as reported in the literature when superimposed in the present flow-pattern map. For this, the following theoretical and empirical models proposed to predict phase inversion in horizontal pipes and stirred vessels have been considered in the present study.

Arirachakaran et al.[5] have suggested an empirical model based on a number of experimental studies on oil−water dispersed flows covering a wide range of oil viscosities, to confirm the importance of viscosity on phase inversion. The model equation is given below:

$$\epsilon_W^I = \left(\frac{U_{sw}}{U_m}\right)_I = 0.5 - 0.1108 \log_{10}(\eta_o/\eta_r) \tag{5}$$

In the above equation, ϵ_W^I is the critical water cut for phase inversion, $\eta_r = 1$ m Pa s, η_o is the oil viscosity, and U_{sw} and U_m are the water superficial and mixture velocities, respectively.

Tidhar et al.[28] have suggested phase inversion occurs at the point where the surface energies of the two possible dispersions (oil dispersed in water and water dispersed in oil) are equal. This has been used with considerable success by Brauner and Ullmann[17] for liquid−liquid flow through horizontal pipes. On the basis of this, they have proposed the following simplified correlation for critical oil holdup for the prediction of phase inversion.

$$\epsilon_o^I = \frac{\bar{\rho}\bar{v}^{0.4}}{1 + \bar{\rho}\bar{v}^{0.4}} \tag{6}$$

where $\bar{v} = \nu_o/\nu_w$ is the kinematic viscosity ratio (oil over water) and $\bar{\rho} = \rho_o/\rho_w$ is the density ratio (oil over water).

Yeh et al.[37] have also suggested a model to predict the phase-inversion point as

$$\epsilon_w^I = 1/(1 + (\eta_o/\eta_w)^{0.5}) \tag{7}$$

This was developed with reference to a configuration of laminar flow in a stratified layer, but its validity was tested against the critical holdup data obtained in a flask (dispersion prepared by manual vigorous shaking of specified volumes of an organic and water phases).

The above-mentioned three models for detection of the phase-inversion point have been superimposed in the present flow-pattern map in Figure 12. In the figure, curves a, b, and c denote

the predictions of eqs 5, 6, and 7, respectively. The curves are observed to lie close to one another and predict almost similar conditions of phase inversion under the present condition of study. All of them are located in the bubbly churn transition at low to moderate flow rates and coincide with the churn-annular transition at high water velocities. This shows that the curves predicting phase inversion appear to depict a situation where the dominating phase shifts from water to kerosene or vice versa. At high water velocity, water remains as the predominant phase over a larger range of kerosene velocities as expected and the onset of "core annular flow" marks phase inversion. Thus, phase inversion represents a transition from a flow pattern with water as the continuous phase to a distribution where kerosene is predominant in the flow passage. The distribution after phase inversion represents a chaotic mixture of two phases with a changeover of the continuous medium at low to moderate flow rates of water and core annular flow at high water velocities.

4. Conclusions

A novel nonintrusive optical probe has been designed and fabricated in the present work to identify the flow patterns during two-phase kerosene−water flow through a vertical pipe. The device is based on the difference in optical properties of the two fluids and can distinguish between dispersed and separated flows on the basis of the fraction of light attenuated and scattered by the two-phase medium. The normalized time-series data of the optical probe has been analyzed by PDF and wavelet analysis. The analysis has shown that, at low flow rates of both the phases, kerosene flows as droplets in the continuous water phase. This flow pattern has been named as bubbly flow in convention to gas−liquid flows. At a high flow rate of kerosene, the signal analysis shows that there exists a core annular flow pattern with kerosene flowing as a core and the water occupying the annular space between the kerosene core and the pipe wall. The transition from bubbly to annular flow has been observed to proceed through a flow pattern consisting of a chaotic distribution of the two phases where the dominating phase shifts from water to kerosene. This flow pattern resembles the churn flow pattern of gas−liquid flows. The range of existence of the different flow patterns has been represented as a flow-pattern map where the bubbly dispersed bubbly transition occurs in accordance to the homogeneous model proposed by Brauner.[35] The bubbly churn transition occurs when the ratio of the inlet flow rate of oil to total mixture velocity lies within 0.2−0.3 and is governed by eq 2. The churn−annular transition is governed by eq 3 at low water flow rates, according to the flooding criteria proposed by Wallis[36] for gas−liquid flows.

Acknowledgment

The authors gratefully acknowledge the partial financial support by the Department of Science and Technology of India.

Literature Cited

(1) Russell, T. W. F.; Charles, M. E. The effect of the less viscous liquid in the laminar flow of two immiscible liquids. *Can. J. Chem. Eng.* **1959**, *37*, 18.

(2) Charles, M. E.; Govier, G. W.; Hodgson, G. W. The horizontal pipeline flow of equal density oil−water mixture. *Can. J. Chem. Eng.* **1961**, *39*, 27.

(3) Hasson, D.; Mann, U.; Nir, A. Annular flow of two immiscible liquids. I. Mechanisms. *Can. J. Chem. Eng.* **1970**, *48*, 514.

(4) Guzhov, A.; Grishin, A. D.; Medredev, V. F.; Medredeva, O. P. Emulsion formation during the flow of two liquids in a pipe. *Neft Khoz* **1973**, *8*, 58 (in Russian).

(5) Arirachakaran, S.; Oglesby, K. D.; Malinowsky, M. S.; Shoham, O.; Brill, J. P. An analysis of oil/water flow phenomena in horizontal pipes. Presented at SPE Production Operating Symposium, Oklahoma, March 1989; SPE Paper 18836, p 155.

(6) Angeli, P.; Hewitt, G. F. Flow structure in horizontal oil−water flow. *Int. J. Multiphase Flow* **2000**, *26*, 1117.

(7) Vigneaux, P.; Chenais, P.; Hulin, J. P. Liquid−liquid flows in an inclined pipe. *AIChE J.* **1988**, *34*, 781.

(8) Jin, N. D.; Nie, X. B.; Ren, Y. Y.; Liu, X. B. Characterization of oil/water two-phase flow patterns based on nonlinear time series analysis. *Flow Meas. Instrum.* **2003**, *14*, 169.

(9) Ioannou, K.; Hu, B.; Matar, O. K.; Hewitt, G. F.; Angeli, P. Phase inversion in dispersed liquid−liquid pipe flows. Presented at 5th International Conference on Multiphase Flow, ICMF'04, Yokohama, Japan, May 30−June 4, 2004; Paper No. 108.

(10) Lovick, J.; Angeli, P. Experimental studies on the dual continuous flow pattern in oil−water flows. *Int. J. Multiphase Flow* **2004**, *30*, 139.

(11) Ioannou, K.; Nydal, O. J.; Angeli, P. Phase inversion in dispersed liquid−liquid flows. *Exp. Therm. Fluid Sci.* **2005**, *29*, 331.

(12) Jana, A. K.; Das, G.; Das, P. K. Flow regime identification of two-phase liquid−liquid upflow through vertical pipe. *Chem. Eng. Sci.* **2006**, *61*, 1500.

(13) Farrar, B.; Bruun, H. H. A computer based hot-film technique used for flow measurements in a vertical kerosene−water pipe flow. *Int. J. Multiphase Flow* **1996**, *22*, 733.

(14) Hamad, F. A.; Imberton, F.; Brunn, H. H. An Optical Probe for measurement in liquid−liquid two-phase flow. *Meas. Sci. Technol.* **1997**, *8*, 1122.

(15) Hamad, F. A.; Pierscionek, B. K.; Brunn, H. H. A dual optical probe for volume fraction, drop velocity and drop size measurements in liquid−liquid two-phase flow. *Meas. Sci. Technol.* **2000**, *11*, 1307.

(16) Simmons, M. J. H.; Azzopardi, B. J. Drop size distributions in dispersed liquid−liquid pipe flow. *Int. J. Multiphase Flow* **2001**, *27*, 843.

(17) Brauner, N.; Ullmann, A. Modelling of phase inversion phenomenon in two-phase pipe flow. *Int. J. Multiphase Flow* **2002**, *28*, 1177.

(18) Jones, O. C.; Delhaye, J. M. Transient and Statistical Measurement Techniques for Two Phase Flows: A Critical Review. *Int. J. Multiphase Flow* **1976**, *3*, 89.

(19) Jones, O. C.; Zuber, N. The interrelation between void fraction fluctuations and flow pattern in two phase flow. *Int. J. Multiphase Flow* **1975**, *2*, 273.

(20) Vince, M. A.; Lahey, R. T., Jr. On the Development of an Objective Flow Regime Indicator. *Int. J. Multiphase Flow* **1982**, *8*, 93−124.

(21) Ren, J.; Mao, Q.; Li, J.; Lin, W. Wavelet analysis of dynamic behaviour in fluidized beds. *Chem. Eng. Sci.* **2001**, *56*, 981.

(22) Ellis, N.; Briens, L. A.; Grace, J. R.; Bi, H. T.; Lim, C. J. Characterization of dynamic behaviour in gas−solid turbulent fluidized bed using chaos and wavelet analyses. *Chem. Eng. J.* **2003**, *96*, 105.

(23) Ellis, N.; Bi, H. T.; Lim, C. J.; Grace, J. R. Influence of probe scale and analysis method on measured hydrodynamic properties of gas-fluidized beds. *Chem. Eng. Sci.* **2004**, *59*, 1841.

(24) Briens, L. A.; Ellis, N. Hydrodynamics of three-phase fluidized bed systems examined by statistical, fractal, chaos and wavelet analysis methods. *Chem. Eng. Sci.* **2005**, *60*, 6094.

(25) Drahos, J.; Ruzicka, Marek C. Problems of Time Series Analysis in Characterization of Multiphase Flows. Presented at 5th International Conference on Multiphase Flow, ICMF'04, Yokohama, Japan, May 30−June 4, 2004; Paper No. K04.

(26) Takei, M.; Ochi. M.; Horii, K.; Li, H.; Saito, Y. Discrete wavelets auto-correlation of axial turbulence velocity in spiral single-phase flow. *Powder Technol.* **2000**, *112*, 289.

(27) Arashmid, M.; Jeffreys, G. V. Analysis of the phase inversion characteristics of liquid−liquid dispersions. *AIChE J.* **1980**, *26*, 51.

(28) Tidhar, M.; Merchuk, J. C.; Sembira, A. N.; Wolf, D. Characteristics of a motionless mixer for dispersion of immiscible fluids. II. Phase inversion of liquid−liquid systems. *Chem. Eng. Sci.* **1986**, *41*, 457.

(29) Hu, B.; Angeli, P.; Matar, O. K.; Hewitt, G. F. Prediction of phase inversion in agitated vessels using a two-region model. *Chem. Eng. Sci.* **2005**, *60*, 3487.

(30) Liu, L.; Matar, O. K.; Perez de Ortiz, E. S.; Hewitt, G. F. Experimental investigation of phase inversion in a stirred vessel using LIF. *Chem. Eng. Sci.* **2005**, *60*, 85.

(31) Yeo, L. Y.; Matar, O. K.; Perez de Ortiz, E. S.; Hewitt, G. F. A description of phase inversion behaviour in agitated liquid−liquid dispersions under the influence of the Marangoni effect. *Chem. Eng. Sci.* **2002**, *57*, 3505.

(32) Miesen, R.; Beijnon, G.; Duijvestijn, P. E. M.; Oliemans, R. V. A.; Verheggen, T. Interfacial Waves in Core-Annular Flow. *J. Fluid Mech.* **1992**, *238*, 97.

(33) Brauner, N. On the relations between two-phase flows under reduced gravity and earth experiment. *Int. Commun. Heat Mass Transfe*r **1990**, *17*, 271.

(34) Beretta, A.; Ferrari, P.; Galbiati, L.; Andreini, P. A. Horizontal oil−water flow in small diameter tubes. Flow patterns. *Int. Commun. Heat Mass Transfe*r **1997**, *24*, 223.

(35) Brauner, N. The prediction of dispersed flows boundaries in liquid−liquid and gas−liquid systems. *Int. J. Multiphase Flow* **2001**, *27*, 885.

(36) Wallis, G. B. *One-Dimensional Two-Phase Flow*; McGraw-Hill: New York, 1969.

(37) Yeh, G.; Haynie, F. H., Jr.; Moses, R. E. Phase−volume relationship at the point of phase inversion in liquid dispersions. *AIChE J.* **1964**, *102*, 260.

Received for review November 14, 2005
Revised manuscript received January 10, 2006
Accepted January 27, 2006

IE051257E